

# Evaluation of Applied Force During Nasopharyngeal Swab Sampling Using Handheld Sensorized Instrument

Chaewon Park, Ingu Choi, Juhyeong Roh, So Yun Lim, Sung-Han Kim, Jongwon Lee, Sungwook Yang,  
*Member, IEEE*

**Abstract**—Nasopharyngeal swab is the most widely used diagnostic test for COVID-19 detection. However, enormous tests have posed a high risk of infection to medical professionals due to close contact with patients and substantial health burden. While automation of the nasopharyngeal swab is regarded as a potential solution to address these problems, the quantitative study of force for safe and effective control has not been widely performed yet. Hence, this study presents applied force during the standard nasopharyngeal swab sampling procedure using a handheld sensorized instrument. The sensorized instrument can simultaneously measure multi-axis forces and 6-DOF hand motion while allowing natural hand motion as is used in the standard swab sampling. To accurately measure force from the handheld instrument, the compensation of gravity bias is accomplished online while estimating the orientation of the hand with an embedded IMU sensor. As a result, the instrument can measure all three-axes forces by an error below 5 mN. A simulated test on a phantom model using the sensorized instrument shows that how the forces vary during the sampling sequences.

## I. INTRODUCTION

Coronavirus disease 2019 (COVID-19) has spread rapidly and become a global pandemic. While a nasopharyngeal (NP) swab is a reference sampling method to detect severe acute respiratory syndrome coronavirus 2, the procedure may expose medical professionals to a high risk of infection due to close contact with patients. Furthermore, enormous COVID-19 tests lead healthcare burden. Recent studies have suggested that automation of COVID-19 sample collection has great potential to address these issues by performing it in safe and efficient manners [1].

For example, oropharyngeal (OP) swab robots have been proposed. Xie *et al.* introduced a soft robotic approach for OP swab sampling [2]. The clinical evaluation of a semi-automatic OP sampling robot was also conducted regarding controlled force [3]. This robot can move the swab forward automatically until it touches the posterior pharyngeal wall and reaches the pre-set force range. In addition, Wang *et al.* introduced a low-cost miniature robot for NP swab

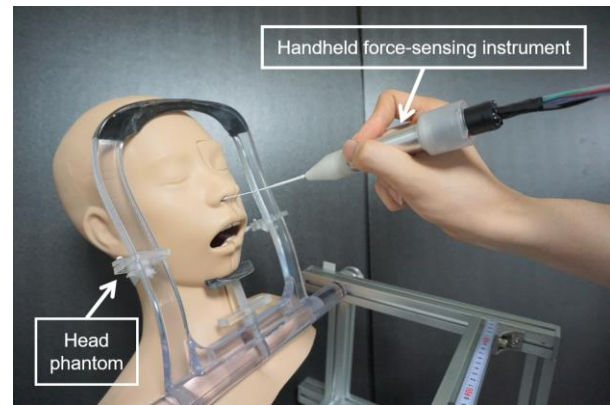


Figure 1. Nasopharyngeal swab sampling with the handheld sensorized instrument.

sampling, which can be controlled by a mobile application [4]. A 3D-printed force sensor was used for acquiring force during NP swab sampling, and its measurement was evaluated in a phantom model and dissected porcine noses. A tele-operated robot incorporating a force sensor was also presented, where force data was used to notify an operator of the swab in contact with an obstacle ahead [5]. However, it is currently used to estimate the presence and softness of an obstacle rather than to quantitatively measure the amount of force.

During these automatic or semi-automatic swab sampling, the management of applied force is essential to safely insert a sampling swab into a nostril and to roll the swab at the nasopharynx without causing any collateral damage. However, the quantitative analysis of force data during the NP swab sampling has not been widely studied yet. Previous studies merely reported the amount of force applied by robotic swab sampling. It lacks whether the applied force would be appropriate in terms of both safety and efficacy. Therefore, we aim to offer a baseline for the design and control of swab sampling robots by collecting force data during the standard NP swab sampling procedure.

Herein, we introduce a handheld sensorized instrument that can simultaneously measure multi-axis forces and 6-degrees-of-freedom (6-DOF) motion while accommodating a standard NP swab, as shown in Fig. 1. The handheld instrument allows natural hand motion as is used in the routine swab sampling done by medical professionals. However, measuring force accurately from the sensor attached to the handheld instrument is challenging because measured force varies upon the orientation of the instrument even without any interaction with tissues. The sensor attached to such a floating base inevitably suffers from gravity bias led by the inherent weights of the sensor and the NP swab with the varying

\*This research was supported by Korea Advanced Research Program through the National Research Foundation of Korea (NRF) funded by Ministry of Science and ICT (2020M3H8A1115027).

C. Park, I. Choi, J. Lee, and S. Yang are with the Center for Intelligent and Interactive Robotics, Korea Institute of Science and Technology, Seoul, 02792, Korea (corresponding author to provide phone: 82-2-958-5747; fax: 82-2-958-5304; e-mail: swyang@kist.re.kr).

J. Roh is with the Division of Robotics Engineering, Kwangjuon University, Seoul, 01897, Korea.

S. Y. Lim and S.- H. Kim are Department of Infectious Diseases, Asan Medical Center, University of Ulsan College of Medicine, Seoul, 05505, Korea.

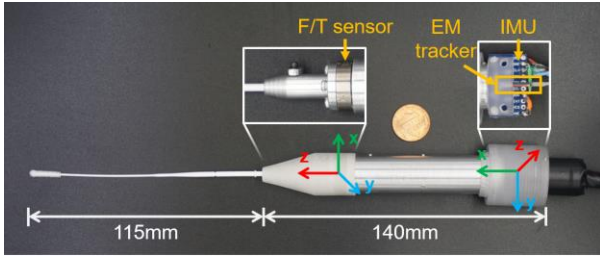


Figure 2. Handheld sensorized instrument with the force/torque sensor, IMU, and EM motion tracker.

orientation of the instrument. A common method compensating for the gravity bias is to estimate the orientation of moving sensors from the kinematics of grounded robot manipulators, given known weight loaded on the sensors [6]. Kim *et al.* also proposed a method to compensate for force/torque offsets using an ANN model with a 9-DOF IMU sensor embedded into a custom-built force sensor [7].

To compensate for force bias from the ungrounded handheld instrument, we propose a least-squares method that can simultaneously find the initial sensor offsets and effective weight loaded onto the sensor, using an IMU sensor integrated into the instrument. Given the sensorized instrument, we perform the quantitative analysis of applied force over the procedure of nasopharyngeal swab sampling with the hand motion trajectory in a phantom model.

## II. MATERIALS AND METHODS

### A. Handheld Sensorized Instrument

The handheld sensorized instrument consists of a 6-axis force/torque sensor (Nano-17, ATI Industrial Automation Inc., USA), an IMU sensor (MPU-9250, InvenSense Inc., USA), an electromagnetic (EM) tracker (VIPER™ with Micro Sensor 1.8™, Polhemus, USA), and a handpiece held by an operator. The force sensor is attached to the handpiece's proximal end, and a swab adaptor is fabricated to connect a standard NP swab to the sensor. The sample collecting swab can easily be loaded into the instrument and replaced by a sliding fit. The 9-DOF IMU sensor placed at the distal end allows the retrieval of the instrument's orientation from a 3-axis accelerometer, a 3-axis gyroscope, and a 3-axis magnetometer. In addition, the EM tracker attached to the handpiece measures the operator's 6-DOF hand motion during nasopharyngeal swab sampling. The instrument is 140 mm long, and its diameter is 19 mm as shown in Fig. 2. The total weight of the instrument is 48.5 g.

For real-time data processing and logging, we build a high-speed sensing interface. A main control board is interfaced with a daughterboard via SPI communication, designed for high-speed six-channels analog-to-digital

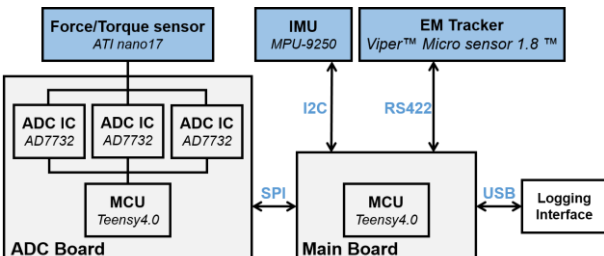


Figure 3. Control diagram of the handheld sensorized instrument.

converting (AD7732, Analog Devices, Inc., USA) of force sensor signals. The 9-DOF IMU sensor is interfaced directly with the main control board through an I2C protocol. Given the IMU data, the main control board estimates the orientation of the instrument using an IMU and AHRS sensor fusion algorithm (orientation filter for inertial/magnetic sensor arrays [8]). The gravity bias of the force sensor is then compensated online for the current orientation of the instrument. The instrument's position and orientation from the EM tracker are streamed into the main controller by RS-422 communication. All sensor data are sampled and synchronized at 500 Hz in the main controller run by a microcontroller (Teensy 4.0 with ARM Cortex-M7 at 600 MHz, PJRC, USA). Finally, all synchronized data are delivered to a PC via USB communication. A custom-built graphical user interface (GUI) was also developed to display force and tracker position in real-time and record the sensing data for further analysis.

### B. Gravity Compensation Using IMU

To obtain unbiased force in real-time, we eliminate the sensor's initial offsets and varying gravity bias led by the orientation change of the sensor. Force  $F_m$  measured by the sensor involves unbiased force  $F_u$ , initial bias  $F_b^0$  by static offsets, and gravity bias  $F_b^g$  by its weight as in (1).

$$F_m = F_u + F_b^0 + F_b^g \quad (1)$$

The initial bias is rather static and described as a fixed value, whereas the gravity bias varies substantially upon the sensor's orientation change. The varying gravity bias is described by the rotation of the instrument  $Rot_{IMU}$  and gravity force  $f_g$  yielded by the weights of the sensor and the NP swab loaded:

$$F_b^g = TR_{IMU}^{Sensor} Rot_{IMU} \begin{bmatrix} 0 \\ 0 \\ -f_g \end{bmatrix}, \quad (2)$$

where  $TR_{IMU}^{Sensor}$  is a coordinate transformation from the IMU and to the force sensor frames as indicated in Fig. 2. Since the first and second elements of the gravity vector are zero, the gravity bias is further simplified as in (3).

$$F_b^g = \begin{bmatrix} 0 & 0 & R_x \\ 0 & 0 & R_y \\ 0 & 0 & R_z \end{bmatrix} \begin{bmatrix} 0 \\ 0 \\ -f_g \end{bmatrix} \quad (3)$$

$R_x$ ,  $R_y$ ,  $R_z$  are the third column vector of the  $TR_{IMU}^{Sensor} Rot_{IMU}$ . Without any external load except the gravity ( $F_u \approx 0$ ), the measured force  $F_m$  comprises only the initial bias  $F_b^0$  and the gravity bias  $F_b^g$ , which can be formulated as in (4).

$$\begin{bmatrix} F_{mx} \\ F_{my} \\ F_{mz} \end{bmatrix} = \begin{bmatrix} F_{bx}^0 + F_{bx}^g \\ F_{by}^0 + F_{by}^g \\ F_{bz}^0 + F_{bz}^g \end{bmatrix} = \begin{bmatrix} 1 & 0 & 0 & -R_x \\ 0 & 1 & 0 & -R_y \\ 0 & 0 & 1 & -R_z \end{bmatrix} \begin{bmatrix} F_{bx}^0 \\ F_{by}^0 \\ F_{bz}^0 \\ f_g \end{bmatrix}, \quad (4)$$

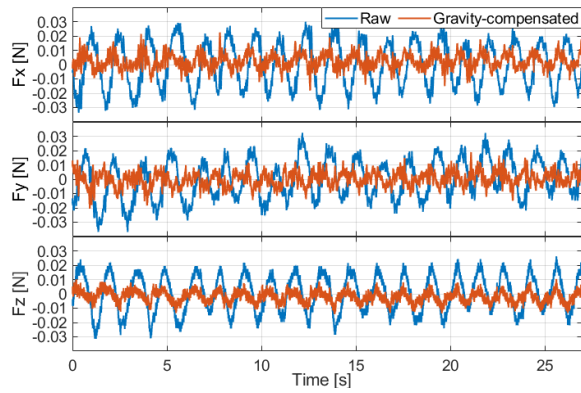


Figure 4. Raw versus gravity-compensated force profiles upon orientation changes under no load.

Hence, our goal is to find four unknown values—three sensor offsets  $F_{bx}^0$ ,  $F_{by}^0$ , and  $F_{bz}^0$ , and the gravity force  $f_g$ . Given the instrument's rotation about an arbitrary axis, multiple measurements of force and handle orientation obtained by the IMU are collected. By vertically cascading (4) for the multiple measurements, we obtain the least-squares solution of  $F_{bx}^0$ ,  $F_{by}^0$ ,  $F_{bz}^0$ , and  $f_g$ . Finally, the unbiased force  $F_u$  is calculated by eliminating the bias  $F_b^0$  and  $F_b^g$  from (1).

Fig. 4 shows raw force profiles fluctuating due to the gravity bias (shown in the blue) for the rotational motion of the wrist without external load. For comparison with compensated force data, the initial values of the sensor offset and gravity bias are eliminated by zeroing the baseline of the sensor data at the beginning of data collection. The compensated force profiles (shown in the red) significantly lower the force fluctuation. The root-mean-square error (RMSE) and maximum error of force data are calculated and summarized in Table I. Overall errors were reduced by 62–69% in the RMSEs for the  $x$ -,  $y$ -, and  $z$ -axes forces. Specifically, the maximum error of the  $z$ -axis force substantially decreased from 0.031 N to 0.005 N.

### III. EXPERIMENTS AND RESULTS

#### A. Phantom Experiment

We measured applied force during the nasopharyngeal

TABLE I  
EVALUATION GRAVITY COMPENSATION

Axis	Raw		Gravity-compensated		Error Reduction
	RMSE (N)	Max. Error (N)	RMSE (N)	Max. Error (N)	
x	0.016	0.032	0.005	0.011	66.67%
y	0.014	0.032	0.005	0.011	62.22%
z	0.013	0.031	0.004	0.005	69.29%

swab sampling procedure using the handheld sensorized instrument in a phantom model (LM097, Suction Training Model Type II, Koken Co. Ltd., Japan). A flocked swab (FLOQSwabs<sup>®</sup>, Copan Diagnostics Inc., USA) used for the standard NP swab was loaded onto the sensorized instrument. A medical professional trained for the NP swab was instructed to perform the NP swab on the phantom model while holding the sensorized instrument in place of the collection swab. The tests were repeated for 20 trials, and all force data with the operator's hand motion were simultaneously recorded.

#### B. Analysis of Applied Force During NP Swab

Fig. 5 shows representative force profiles over the time of NP swab sampling, of which the procedure is divided into four steps [9]. The  $z$ -axis force is shown mostly as negative (compressive) because the upward direction of the sensor's  $z$ -axis heads toward the swab's distal end. First, the swab was inserted into the phantom's nostril—step (I). During this step, the forces on the  $x$ -,  $y$ -, and  $z$ -axes gradually increased due to friction while passing through the nasal floor. At the moment of contact—step (II), the  $z$ -axis force steeply increased as the operator kept pushing the swab toward the nasopharyngeal wall. Once the swab reached the nasopharyngeal wall, the operator gently rotated the instrument for multiple turns to obtain specimens in step (III). All  $x$ -,  $y$ -,  $z$ -axes forces oscillated upon the rotation of the instrument, while 6.5 turns were made on average. The deviation of the  $z$ -axis forces was pronounced compared with the other axes. It is noted that maintaining consistent contact force would be difficult while pivoting the bent tip at the point of contact. Upon completion of specimen sampling, the swab was withdrawn from the phantom's nostril—step (IV). During this step, the positive  $z$ -axis force was occasionally observed as the bent swab reverted to its original form. The total elapsed time for the

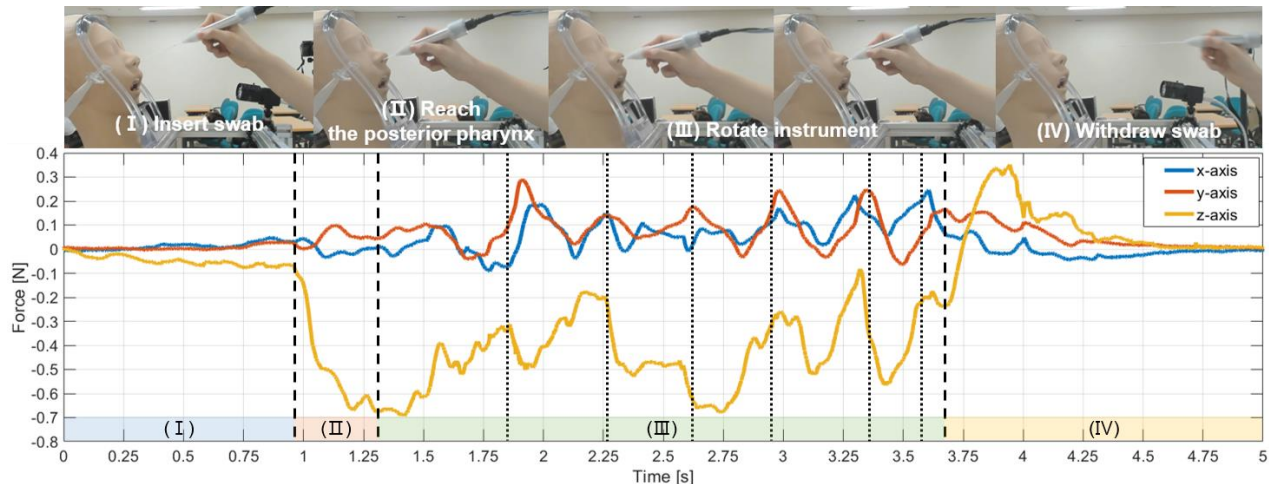


Figure 5. Force profiles during the course of nasopharyngeal swab sampling: (I) insert the swab into the nostril, (II) reach the nasopharynx, (III) roll the instrument, and (IV) withdraw the swab.

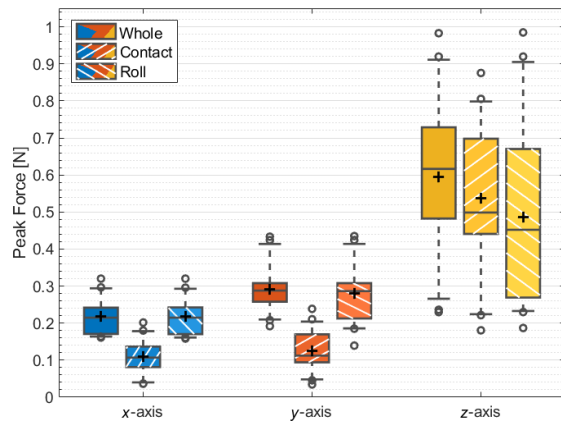


Figure 6. Peak forces detected during the entire procedure (solid), the contact step (45°-hatched), and the roll step only (135°-hatched). A horizontal line and a cross within the rectangle represent the median and the mean of all values, respectively.

entire NP swab procedure was 6.20 s on average. The elapsed times were 2.43, 2.71, and 1.07 s for step (I-II), step (III), and step (IV), respectively.

The solid boxes of Fig. 6 show the maximum peak force for each axis during the entire procedure (through the steps (I) to (IV)). In addition, boxes with 45°- and 135°-hatched angles present the peak forces obtained during steps (II) and (III), respectively. As a result, the maximum peak force on the z-axis was 0.596 N on average, which was 2.0–2.7 times higher than those of the x- and y-axes (0.217 N and 0.291 N, respectively). For the z-axis, the peak force during the contacting step (II) was higher than the peak force during the rotating step (III). On the other hand, the peak forces of the x- and y-axes significantly increased during the rotating step, compared with those of the contacting step.

### C. Analysis of Applied Force with Hand Motion

We also analyzed the applied force regarding the hand motion during the procedure. Fig. 7(a) presents a representative hand trajectory overlaid on a 3D head model, where the magnitude of the force is color-coded with a range of 0.0–0.7 N. Hence, one can identify where force concentration occurs during swab sampling, although the rigid body motion of the instrument was assumed, excluding the tip bending. Fig. 7(b) shows a force-displacement curve for the z-axis force, which was most noticeable during the procedure. The contact to the nasopharyngeal wall is detected at 74 mm posterior from the nostril after passing through the nasal floor. The contact force kept increasing by pushing the swab further toward the nasopharyngeal wall approximately by 6 mm, resulting in a 0.6-N increment. The rotating and rubbing and motion at step (III) led the instrument held by the hand to move back and forth at the sagittal plane, which was 8 mm along the z-axis for a force fluctuation of -0.511–0.055 N.

## IV. DISCUSSION

This study presented applied force during the NP swab sampling procedure using the handheld sensorized instrument developed. The sensorized instrument held by an operator allows to simultaneously measure the multi-axis force and 6-DOF hand motion without changing the standard swab sampling procedure and clinical settings. The online gravity compensation algorithm enables us to measure unbiased force

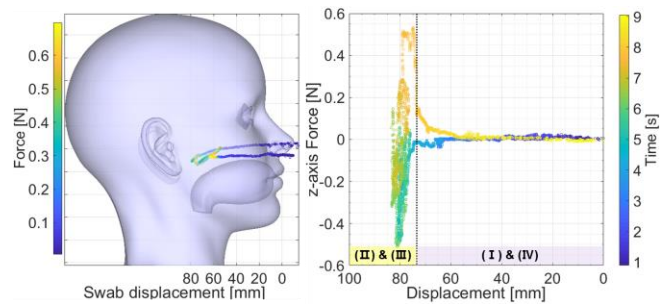


Figure 7. (a) Force during the swab sampling motion. (b) Z-axis force for the swab displacement during the sampling procedure.

accurately from the floating handpiece in real-time. Hence, this study shows how the level of force changes over the sub-sequences of the sampling procedure, which offers baselines in designing and controlling automatic swab sampling robots. Specifically, it is important to identify the range of force and to recognize the moment of contact for ensuring safety during such an automated process. For example, the moment of contact could be found by detecting noticeable slope change in the z-axis force rather than by setting a certain single threshold.

Although this pilot study is limited due to the use of the silicone phantom model, the measured force is still valid. The peak force is yielded primarily by the deflection of the flexible swab shaft, resulting from the advancement of the swab until a certain depth regardless of contact materials. Future plans include collecting force and motion data *in vivo* and offering force margin for the safe and effective control of automatic nasopharyngeal swab sampling systems.

## REFERENCES

- [1] G. Z. Yang, B. J. Nelson, R. R. Murphy, H. Choset, H. Christensen, S. H. Collins, P. Dario, K. Goldberg, K. Ikuta, N. Jacobstein, D. Kragic, R. H. Taylor, and M. McNutt, “Combating COVID-19-The role of robotics in managing public health and infectious diseases,” *Sci. Robot.*, vol. 5, no. 40, pp. 1–3, 2020.
- [2] B. Z. Xie, B. Chen, J. Liu, F. Yuan, Z. Shao, H. Yang, A. G. Domel, J. Zhang, and L. Wen, “A New Way to Collect Sputa Samples ©,” pp. 2–11, 2021.
- [3] S. Q. Li, W. L. Guo, H. Liu, T. Wang, Y. Y. Zhou, T. Yu, C. Y. Wang, Y. M. Yang, N. S. Zhong, N. F. Zhang, and S. Y. Li, “Clinical application of an intelligent oropharyngeal swab robot: Implication for the COVID-19 pandemic,” *Eur. Respir. J.*, vol. 56, no. 2, 2020.
- [4] S. Wang, K. Wang, H. Liu, and Z. Hou, “Design of a low-cost miniature robot to assist the COVID-19 nasopharyngeal swab sampling,” *arXiv*, vol. 3, no. 1, pp. 289–293, 2020.
- [5] J. Seo, S. Shim, H. Park, J. Baek, J. H. Cho, and N. H. Kim, “Development of robot-assisted untact swab sampling system for upper respiratory disease,” *Appl. Sci.*, vol. 10, no. 21, pp. 1–15, 2020.
- [6] Y. Yu, R. Shi, and Y. Lou, “Bias Estimation and Gravity Compensation for Wrist-mounted Force/Torque Sensor,” *IEEE Sens. J.*, 2021, *early access*.
- [7] Y. B. Kim, D. Y. Seok, S. Y. Lee, J. Kim, G. Kang, U. Kim, and H. R. Choi, “6-Axis Force/Torque Sensor with a Novel Autonomous Weight Compensating Capability for Robotic Applications,” *IEEE Robot. Autom. Lett.*, vol. 5, no. 4, pp. 6686–6693, 2020.
- [8] S. O. H. Madgwick, A. J. L. Harrison, and R. Vaidyanathan, “Estimation of IMU and MARG orientation using a gradient descent algorithm,” *IEEE Int. Conf. Rehabil. Robot.*, 2011.
- [9] E. Coden, F. Russo, A. D. Arosio, P. Castelnuovo, A. Karligkiotis, and L. Volpi, “Optimum Naso-oropharyngeal Swab Procedure for COVID-19: Step-by-Step Preparation and Technical Hints,” *Laryngoscope*, vol. 130, no. 11, pp. 2564–2567, 2020.